

Thermodynamic analysis for growth of transition-metal nitride thin films by pulsed laser deposition

Myung-Bok Lee*

Department of Mechanical and Metallic Mold Engineering, Gwangju University, Gwangju 61743, Korea

Thermodynamic analysis has been carried out for growth of transition-metal nitride thin films by pulsed laser deposition. TiN films with (200) orientation were grown on Si(100) substrate without any oxide impurity phase formation at substrate temperature in the range of 20~700 °C. However, polycrystalline ZrN films mixed with ZrO₂ phase were grown at 550~700 °C at the same deposition conditions. We prepared the diagram of chemical potential of nitrogen (μ_{N_2}) with variation of temperature for the nitride films and the P_{O_2} - P_{N_2} phase diagram for Ti and Zr at 973 K. We could expect from the thermodynamic diagram that ZrO₂ phase tends to be more easily formed at 700 °C than TiO₂ phase during the nitride film growth at the same gas atmosphere, as is consistent with experimental results. Formation and phase stability of TiN and ZrN films at elevated temperatures are systematically analyzed and compared to each other.

Key words: Nitride films, Transition metal nitride, Thermodynamics, μ -T diagram, Phase stability.

Introduction

Nitride thin films have been attracting much interests because of their wide spectrum of physical properties and applicability. They exhibit an insulating nature (e.g. Si₃N₄), wide-gap semiconducting properties (e.g. AlN, GaN, InN), and metallic conducting properties (e.g. TiN, ZrN). Especially, transition metal nitrides with NaCl structure, such as TiN and ZrN, have high electrical conductivity, together with high chemical stability, hardness, and abrasion resistance. Hence, they have found many applications not only as a wear- and abrasion-resistant coating material but also as a diffusion barrier for metallization and contact formation in VLSI process technologies [1-4]. TiN and ZrN films have been deposited by various methods such as CVD [5], ion plating [6], reactive magnetron sputtering [7], pulsed laser deposition (PLD) [8], and atomic layer deposition (ALD) [9].

To interpret the characteristics of reaction systems and design the reaction process more easily, thermodynamic analysis is required in metal nitride thin film deposition as well as in oxide deposition [10, 11]. The chemical potential(μ) vs temperature(T) diagram (ΔG^0 - T phase diagram), known as Ellingham diagram, is convenient to describe the oxidation and reduction equilibrium of various oxide systems at high temperatures. The μ - T diagram for some nitridation reaction exists, however, that for various transition

nitrides has not been prepared systematically [12].

In this paper, we describe the preparation of μ - T diagram for nitride materials and discuss the formation and phase stability of nitrides at elevated temperatures. We apply the diagram for the formation of TiN and ZrN films grown by PLD and analyze the results by thermodynamic consideration.

Experimental

TiN and ZrN films were grown on Si(100) substrates by PLD. Fig. 1 shows the schematic diagram of PLD apparatus used for the deposition of films. A KrF excimer laser (Lambda Physik, LPX100) with 248 nm wavelength and 20 ns pulse width was used to ablate

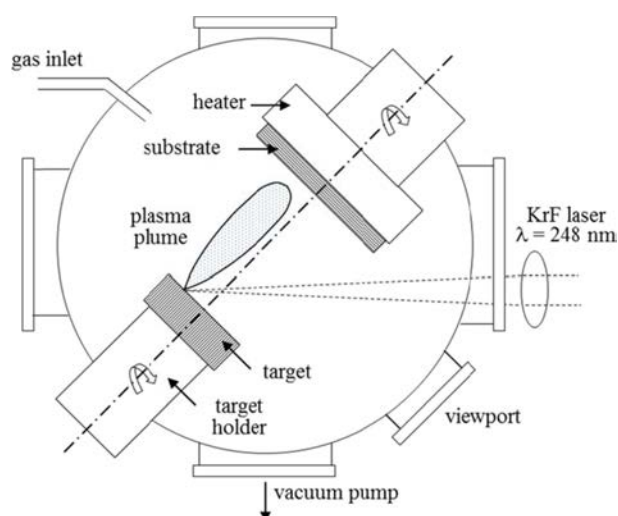


Fig. 1. Schematic diagram of pulsed laser deposition apparatus.

*Corresponding author:
 Tel : +82-62-670-2692
 Fax: +82-62-670-2698
 E-mail: mblee3@gwangju.ac.kr

hot-pressed stoichiometric TiN and ZrN targets (Cerac, 99.9% purity) with 10-20 mm diameter. The repetition rate of laser shot was 5 Hz and laser energy fluence was 2-3 J/cm². The target was rotated at a period of 5 seconds to reduce the crater formation on the surface. The chamber was evacuated to $\sim 10^{-7}$ Torr by a turbomolecular pump with the aid of a rotary pump. The substrate-target distance was fixed at 35 mm. A Si wafer cut by 10×10 mm² size was ultrasonically cleaned in acetone and isopropyl alcohol, dipped into 5% HF solution to remove the natural oxide film, rinsed with pure water and dried with N₂ gas blow, and fixed onto a heater block. Substrate temperature was varied from room temperature to 700 °C. Deposition was carried out either in vacuum ($\sim 10^{-6}$ Torr) without the introduction of atmosphere gas or in high-purity N₂ with a partial pressure of 1 and 10 mTorr. After the film deposition, the sample was slowly cooled down to room temperature in the chamber to avoid the oxidation of the films. The crystal structure of the films was analyzed by $2\theta/\theta$ X-ray diffractometer (Mac Science, MXP3) using a graphite monochromator and a Ni filter to select the CuK α line.

Results and Discussion

Fig. 2 shows the XRD patterns of TiN films deposited on Si(100) substrates at various substrate temperatures in vacuum. The TiN single phase was formed without any oxide phase formation in a wide range of temperature. While TiN(111) peak intensities remained very weak, TiN(200) peak intensities became stronger with the increase of substrate temperature. At 700 °C, TiN film with a strong (200) orientation was deposited. The FWHM of the TiN(200) peak was as low as 1.35°, showing very high crystallinity of the TiN film deposited at 700 °C. The variation of deposition atmosphere from high vacuum to N₂ pressure of 1 and 10 mTorr showed little change in the TiN(200) peak intensity. Fig. 3 shows the XRD patterns of ZrN films deposited on Si(100) substrates at various substrate temperatures in vacuum. The formation of crystalline phases and crystal orientation in ZrN film deposition strongly depended on the substrate temperature. The single phase of ZrN was obtained at temperatures lower than 450 °C. Oxide phase started to grow with increase of the substrate temperature, resulting in mixed phases of ZrN and ZrO₂ at temperatures higher than 550 °C. The crystalline phase of ZrO₂ changed from monoclinic to tetragonal structure as substrate temperature increased. The optimum temperature for the growth of a ZrN film with a strong (200) orientation was 450 °C, which was much lower than that of TiN. We have also deposited ZrN films in N₂ gas of 1 and 10 mTorr at the substrate temperature of 450 °C, and found that the intensities of the ZrN(200) peaks prepared in N₂ atmosphere were slightly lower than that of the films prepared in

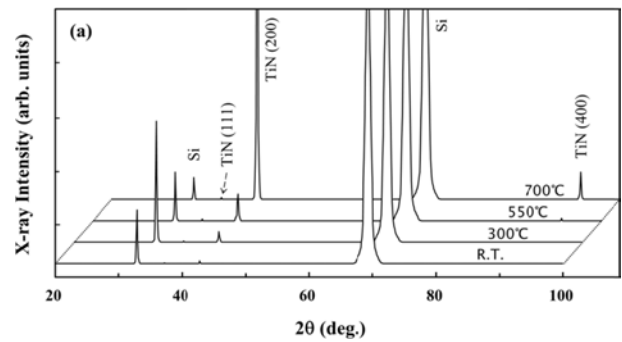


Fig. 2. XRD patterns of TiN films deposited on Si(100) substrate at various substrate temperatures.

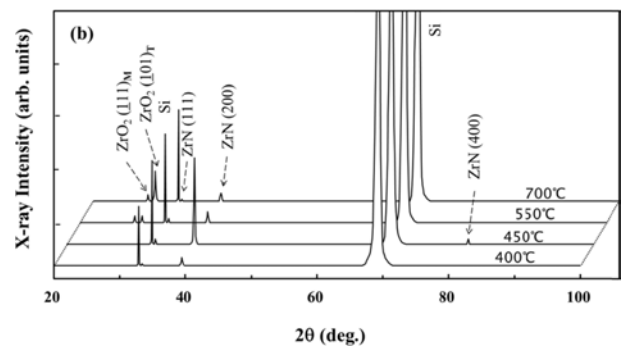


Fig. 3. XRD patterns of ZrN films deposited on Si(100) substrate at various substrate temperatures. The subscript of M and T for ZrO₂ denotes monoclinic and tetragonal phase, respectively.

vacuum.

Thermodynamically, it is favorable that thin film growth occurs to make the plane of lowest free energy, i.e. the most closely packed plane, orients parallel to the substrate surface to reduce the number of dangling bonds. The crystal plane of lowest free energy is (200) in transition metal nitride films with the NaCl structure. The increase of the X-ray intensity of (200) peak relative to that of (111) peak was observed in TiN films with increase of the substrate temperature. This is because the higher substrate temperature will help the film to take a structure close to that in thermodynamic equilibrium.

We describe the preparation of the μ - T diagram to estimate the formation and phase stability of nitrides at elevated temperatures. Let's consider the nitridation reaction for a metal M to form a metal nitride MN as follows:



When the reaction is in equilibrium, Gibbs free energy change (ΔG) obeys the following relation:

$$\Delta G = \Delta G_f^0 + RT \cdot \ln K = \Delta G_f^0 + RT \cdot \ln [a_{MN}^2 / (a_M^2 \cdot P_{N_2})] \quad (2)$$

where ΔG_f^0 is the Gibbs free energy change for nitride formation at standard state (1 atm), R is the gas constant, T is the temperature, K is the reaction constant, and a is the activity, and P is the pressure. Since the activities of solids are equal to unity, equation (2) becomes,

$$\Delta G = \Delta G_f^0 - RT \cdot \ln P_{N_2} \quad (3)$$

When M and MN are in equilibrium state, ΔG must be zero. Therefore,

$$\Delta G_f^0 = RT \cdot \ln P_{N_2} = \Delta H_f^0 - T \cdot \Delta S_f^0 \quad (4)$$

where ΔH_f^0 and ΔS_f^0 is the enthalpy change and the entropy change of nitride formation, respectively, at standard state. The ΔH_f^0 and ΔS_f^0 are independent on temperature by first order approximation if there is no phase change of reactants and products, and can be calculated by using thermodynamic data of reactants and products [13, 14]. Thus, if we take the chemical potential of nitrogen

$$\mu_{N_2} = RT \cdot \ln P_{N_2} \quad (5)$$

in longitudinal axis and the temperature in transverse axis, we can determine the coexisting line of M and MN for the reaction shown in equation (1).

Furthermore, the equation (5) can also be written as,

$$\mu_{N_2} = (2.303R \cdot \log P_{N_2}) \cdot T \quad (6)$$

From equation (6), a straight line radiates from the origin ($\mu_{N_2} = 0, T = 0$) and has a slope of $2.303R \cdot \log P_{N_2}$ when $\log P_{N_2}$ has a determined value. Thus, if we add the nomographic scale of $\log P_{N_2}$ in right-hand side of longitudinal axes, we can know the nitrogen partial pressure where any metal and metal nitride are in equilibrium state at any temperature.

For the equilibrium reaction when M is a gas phase, we can consider another reaction,



The chemical potential for equilibrium reaction in this case can be represented as,

$$\begin{aligned} \mu_{N_2} &= RT \cdot \ln P_{N_2} = \Delta G_f^0 + RT \cdot \ln(P_{NH_3}^2/P_{H_2}^3) \\ \Delta G^0 &= -92.22 + 0.199T \text{ (kJ/mole)} \end{aligned} \quad (8)$$

We can add another nomographic scale of $\log(P_{NH_3}^2/P_{H_2}^3)$ in the right-hand side for equilibrium reaction including two gas components. We considered here various nitride formation reactions, calculated and plotted the μ_{N_2} - T diagram as is shown in Fig. 4. If there is a phase change of the reactants or products, such as melting of metal element, the enthalpy and entropy

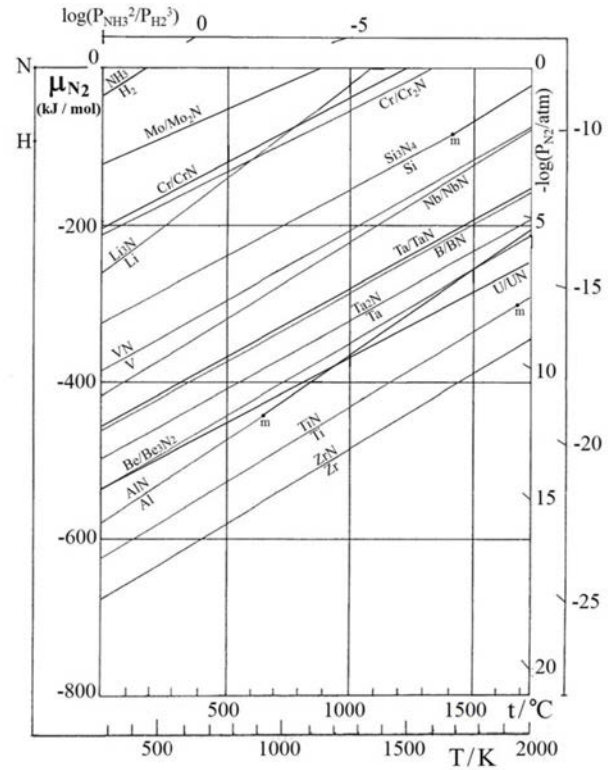


Fig. 4. The μ_{N_2} - T phase diagram prepared for some important nitride materials by calculation using thermodynamic data of materials. The dot 'm' denotes the elemental melting point.

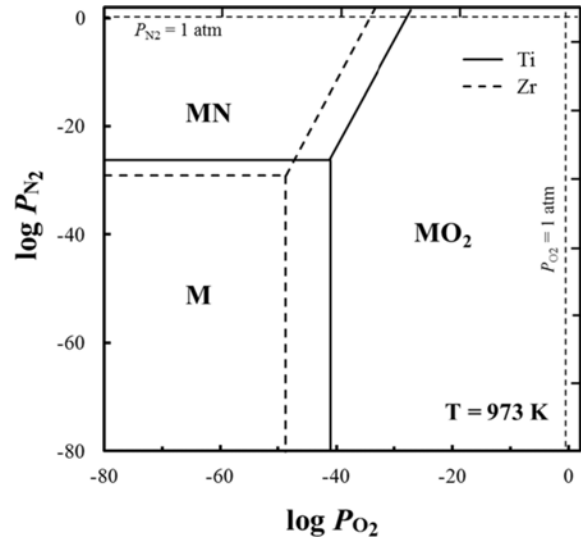


Fig. 5. The P_{N_2} - P_{O_2} phase diagram prepared for Ti, Zr metals and their compounds at $T = 973$ K.

change should be modified in equation (4) as $\Delta H^0 = \Delta H_f^0 - \Delta H_m^0$ and $\Delta S^0 = \Delta S_f^0 - \Delta S_m^0$, where ΔH_m^0 and ΔS_m^0 represents enthalpy change of melting and entropy change of melting, respectively. We marked the melting points of some metal elements in Fig. 4.

When the number of parameters controlling the chemical potential of the system increases, such as in coexisting ambient of oxygen and nitrogen, it is

impossible to describe states of the system in two dimension and we should give a three-dimensional description. If single parameter is fixed, the two-dimensional cross-section of the phase diagram can be obtained in this case. By fixing temperature at $T=973\text{K}$ where our PLD process carried out, we can calculate the formation range of MN and MO_2 phases. In this calculation, we can assume following equilibrium states:

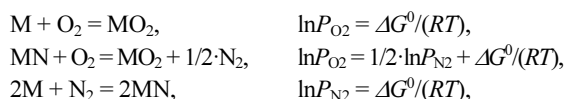


Fig. 5 shows the $\log P_{\text{N}_2}$ - $\log P_{\text{O}_2}$ phase diagram for Ti, Zr metals and their compounds. From the figure, we can see the formation range of ZrO_2 phase is much wider than that of TiO_2 phase, while the formation range of ZrN shows only a little difference with that of TiN. We can easily expect from the diagram that ZrO_2 phase will tend to be more easily formed at 973K than TiO_2 during the nitride film growth, as is consistent with our experimental results.

We have considered the formation and phase stability of metal nitrides in TiN and ZrN film deposition from the viewpoint of thermodynamics. In real situations of thin film growth, considerations of reaction kinetics should be taken into account as well as thermodynamic considerations. In PLD process, when a pulsed laser beam is impinged on a metal nitride target, the surface of the target is ablated to form a plasma plume which contains activated metal and nitrogen atoms and ions. These activated species are almost instantly condensed into a metal nitride film on the substrate. Then, the metal nitride may be oxidized through reaction with the residual oxygen source in the environment during the interval of laser pulses. The oxidation of metals proceeds via the diffusion of either metallic or oxygen ions through the oxide layer. The diffusion coefficient of oxygen in ZrO_2 is known to be much higher ($D \sim 10^{-12} \text{cm}^2/\text{s}$ at 500°C) than that in TiO_2 ($D \sim 10^{-15} \text{cm}^2/\text{s}$ at 800°C) [15, 16]. Therefore, once the oxides are formed at the growing surface of nitride films, ZrO_2 will grow rapidly, especially at higher temperatures, than TiO_2 does. This is also consistent with our observation that TiN phase is stable in the entire temperature range, but ZrN is stable only in the temperature range lower than 450°C .

Conclusions

We systematically analyzed the formation and phase stability of TiN and ZrN films grown by PLD, and described the differences of the two material. Thermodynamic analysis was carried out to estimate the phase stability of the films at elevated temperatures

employing our own thermodynamic diagrams established from thermochemical data of materials. TiN films with (200) orientation were grown on Si(100) substrate without any oxide impurity phase formation. However, polycrystalline ZrN films mixed with ZrO_2 phase were grown at the same deposition conditions. We could expect from the P_{O_2} - P_{N_2} phase diagram that ZrO_2 phase tended to be more easily formed at 700°C than TiO_2 phase does during the nitride film growth at the same gas atmosphere. Reaction kinetics for the growth of oxide phase was also taken into account to interpret the phase stability of grown nitride films.

Acknowledgments

This study was conducted with research funds from Gwangju University in 2018.

References

1. H. Kim, J. Vac. Sci. Technol. B 21[6] (2003) 2231-2261.
2. Y. Liu, S. Kijima, E. Sugimata, M. Masahara, K. Endo, T. Matsukawa, K. Ishii, K. Sakamoto, T. Sekigawa, H. Yamauchi, Y. Takanashi, E. Suzuki, IEEE Trans. Nanotechnol. 5[6] (2006) 723-730.
3. D.-S. Kil, H.-S. Song, K.-J. Lee, K. Hong, J.-H. Kim, K.-S. Park, S.-J. Yeom, J.-S. Roh, N.-J. Kwak, H.-C. Sohn, J.-W. Kim, S.-W. Park, in Symp. VLSI Technology Tech. Dig., June 2006, p.38.
4. V. Barral, T. Poiroux, F. Andrieu, C. Buj-Dufournet, O. Faynot, T. Ernst, L. Brevard, C. Fenouillet-Beranger, D. Lafond, J. M. Hartmann, V. Vidal, F. Allain, N. Daval, I. Cayrefourcq, L. Tosti, D. Munteanu, J. L. Autran, S. Deleonibus, in IEDM Tech. Dig., 2007, p.61.
5. C. J. Carmalt, A. Newport, I. P. Parkin, P. Mountford, A. J. Sealey, S. R. Dubberley, J. Mater. Chem. 13 (2003) 84-87.
6. J.-H. Huang, H.-C. Yang, X.-J. Guo, G.-P. Yu, Surf. Coatings Technol. 195 (2005) 204-213.
7. V. Chawla, R. Jayaganthan, R. Chandra, Mater. Charact. 59[8] (2008) 1015-1020.
8. S. H. Kim, H. Park, K. H. Lee, S. H. Jee, D.-J. Kim, Y. S. Yoon, J. Ceram. Proc. Res. 10[1] (2009) 49-53.
9. S. H. Kwon, O. K. Kwon, J. S. Min, S. W. Kang, J. Electrochem. Soc. 153[6] (2006) G578-G581.
10. T. Hashimoto, H. Koinuma, K. Kishio, Jpn. J. Appl. Phys. 30[8] (1991) 1685-1687.
11. T. Kawai, M. Kanai, H. Tabata, S. Kawai, in "Science and Technology of Thin Film Superconductors" (Plenum, New York, 1989), p.21.
12. T. B. Reed, in "Free Energy of Formation of Binary Compounds" (MIT Press, Cambridge, 1971).
13. K. Fueki, in "Denkikagaku Binran" (Maruzen, Denikagaku Kyokai, 1984) p.27 [in Japanese].
14. M. W. Chase, Jr., C. A. Davis, J. R. Downey, Jr., D. J. Frurip, R. A. McDonald, A. N. Syverud, in "JANAF Thermochemical Tables" (Am. Chem. Soc. and Am. Inst. of Phys. for the Natl. Bur. Stand., New York, 1985), 3rd ed.
15. "Diffusion Data", ed. F. H. Wohlbier (Diffusion Information Center, Cleveland, 1971), Vol.4, p.114.
16. "Diffusion Data", ed. F. H. Wohlbier (Diffusion Information Center, Cleveland, 1971), Vol.5, p.497.